Bol. Soc. Paran. Mat.
©SPM – E-ISSN-2175-1188
SPM: www.spm.uem.br/bspm

(3s.) **v. 2025 (43) 1** : 1–13.
ISSN-0037-8712
doi:10.5269/bspm.78394

A Wavelet-Based Symbolic Method for Time-Space Fractional Advection Equations with Caputo Derivatives

Mutaz Mohammad*, Mohyeedden Sweidan, Alexander Trounev, Praveen Agarwal

ABSTRACT: This paper presents a wavelet-based numerical method for solving time–space fractional advection equations involving Caputo derivatives. The governing equation is given by

$$d_1 \frac{\partial^\beta W}{\partial z^\beta} + d_2 \frac{\partial^\gamma W}{\partial u^\gamma} = h(z,u),$$

where $0 < \beta, \gamma \leq 1$ denote fractional orders in the Caputo sense, and $h(z,u)$ is a known source function. The proposed scheme uses a collocation approach based on Euler wavelets—compactly supported bases constructed from shifted and scaled Euler polynomials. This structure enables an exact symbolic evaluation of fractional derivatives and facilitates accurately enforcing boundary conditions.

The numerical framework builds the solution through coefficient matrices and vector terms derived from a symbolic system, ensuring consistency with the governing equation at carefully selected collocation points. A central result shows that, when the exact solution is polynomial and symbolic computation is used, the method reproduces the solution exactly at all collocation nodes.

Numerical experiments support the theoretical findings, demonstrating high accuracy and computational efficiency, particularly for smooth solutions where rapid convergence is observed. Compared to existing approaches, the method offers enhanced precision and broader applicability, especially for problems involving coupled space–time non-locality. This work expands the use of Euler wavelets in fractional partial differential equations. It provides a mathematically rigorous framework for future extensions to nonlinear and multidimensional problems.

Key Words: Fractional advection equation, Euler wavelets, Caputo fractional derivative, Wavelet collocation method, numerical solution of fractional PDEs, anomalous transport, computational mathematics.

Contents

1. Introduction

Fractional-order models have achieved marked success in the accurate description of transport phenomena that exhibit memory and non-locality—features often mishandled by classical differential approaches constrained to locality and exponential decay, [1,4,12,28,32,7,26]. In contrast, fractional partial differential equations (FPDEs), particularly those employing Caputo-type derivatives, can capture anomalous diffusion characterized by power-law scaling and long-range dependencies. This methodological shift has been deeply explored since Podlubny's foundational work [27] and the comprehensive analysis in [11].

* Corresponding author.
2010 *Mathematics Subject Classification:* 42C40, 65T60, 65M70, 26A33.
Submitted August 13, 2025. Published December 19, 2025

A prominent FPDE in this context is the time–space fractional advection equation, which generalizes classical transport models to include both temporal and spatial fractional orders. Such equations have proven valuable across various applications: anomalous transport in porous and fractured media [16, 8], viscoelastic composite deformation [14,23], and modeling of heterogeneous fluid flow in fractured geological formations and atmospheric strata [30,15]. Using Caputo derivatives, these models retain the ability to pose physically interpretable initial and boundary conditions [6].

One of the key challenges remains the efficient numerical approximation of these inherently nonlocal FPDEs. Wavelet-based methods—utilizing their multiscale, localized properties—have delivered significant advances. In particular, Euler wavelets stand out for their compact support, recursive structure, sparse operational matrices, and symbolic tractability for fractional differentiation [3,13,10]. Their utility has been confirmed in optimal-control formulations of fractional integro-differential systems [2], and time–fractional advection–diffusion problems [31]. Alternative wavelet bases, including Riesz, Daubechies, pseudo-spline, and tight framelet constructions, have been successfully applied to epidemiological dynamics [25,20], neurodegenerative modeling [21], and seismic analysis [17].

More recent developments have extended fractional modeling in promising directions. Unified fractional derivative formulations have improved the treatment of boundary layer physics - [19]. Hybrid frameworks combining fractional operators with data-driven methods have begun to emerge in seismic machine learning applications [17]. Additionally, fractional Riccati systems [18] and neutral delay-fractional equations [22] illustrate the broadening of the theoretical scope.

New numerical strategies continue to surface: barycentric rational-collocation for 2D time-fractional advection–diffusion equations [31], Hermitian-interpolation-based finite-difference schemes for space–time Riesz–Caputo wave equations [9,29], and FFT-accelerated operational-matrix methods using Caputo derivatives [5]. These methods complement wavelet frameworks like Euler wavelets and further enrich the field's computational toolbox.

Consequently, the fractional advection equation of time-space emerges as a versatile modeling platform that synthesizes the memory, nonlocality, and anomalous scaling features central to disordered media, viscoelastic composites, and heterogeneous fluid domains. This study advances this paradigm by developing an Euler-wavelet-based collocation method tailored to time–space FPDEs involving Caputo fractional derivatives. Our approach supports symbolic differentiation, enforces boundary conditions directly, and demonstrates exact recovery of polynomial solutions under collocation, promising a significant step forward in theory and implementation.

2. The Model and its Approximation

In this study, we consider the generalized time–space fractional advection equation given by

$$d_1 \frac{\partial^\beta W}{\partial z^\beta} + d_2 \frac{\partial^\gamma W}{\partial u^\gamma} = h(z,u), \tag{2.1}$$

where d_1 and d_2 are transport coefficients, and $0 < \beta, \gamma \leq 1$ denote the orders of the Caputo fractional derivatives with respect to the spatial variables z and u, respectively. The function $h(z,u)$ represents a known source term. For $\beta = \gamma = 1$, Equation (2.1) reduces to the classical advection equation.

The Caputo fractional derivative of order $\alpha \in (0,1]$ with respect to a variable $x \in \{z,u\}$, for a sufficiently smooth function f, is defined as

$${}^C D_x^\alpha f(x) = \frac{1}{\Gamma(1-\alpha)} \int_0^x \frac{f'(s)}{(x-s)^\alpha}\, ds, \tag{2.2}$$

where $\Gamma(\cdot)$ denotes the Gamma function. This definition assumes the existence of the first derivative of f, and it is particularly suitable for problems with classical initial or boundary conditions.

The model is subject to the following boundary conditions:

$$W(0,u) = k_1(u), \quad W(z,0) = k_2(z), \tag{2.3}$$

where k_1 and k_2 are prescribed boundary functions. The existence and uniqueness of the solution to Equation (2.1) under these conditions are well established in the literature [30].

To approximate the solution within the unit square domain $0 \le z, u \le 1$, we employ an Euler wavelet-based collocation method, as proposed in [23]. The solution is discretized into matrix form using basis-dependent dimensions: M_1 and M_2 are coefficient matrices of size $n_{km} \times n_{km}$, while V_1 and V_2 are vectors of length n_{km}, where $n_{km} = 2^{k-1}m$, with k and m denoting the wavelet level and polynomial degree, respectively. Our implementation demonstrates superior numerical accuracy, achieving zero absolute error in benchmark problems previously addressed in [8,30]. Additionally, our formulation extends prior models by incorporating fractional derivatives in both spatial dimensions, in contrast to earlier studies—such as [24], which treated time-fractional terms only, and [23], which addressed non-fractional Navier–Stokes systems.

The basis vector of Euler wavelets, $\vec{\Psi}(x)$, is defined as

$$E_m(x) = \sqrt{2m+1}\sum_{k=0}^{m}(-1)^{m-k}x^k\binom{m}{k}\binom{k+m}{k}, \tag{2.4}$$

and

$$\psi_{knm}(x) = \begin{cases} 2^{\frac{k-1}{2}}E_m\left(2^{k-1}x - n + 1\right), & \frac{n-1}{2^{k-1}} \le x < \frac{n}{2^{k-1}}, \\ 0, & \text{otherwise.} \end{cases} \tag{2.5}$$

The vector function $\vec{\Psi}(x)$ is constructed by flattening the matrix $\psi_{kij}(x)$, where $i = 1, 2, \ldots, 2^{k-1}$ and $j = 0, 1, \ldots, m-1$. For example, when $k = 2$ and $m = 4$, the vector $\vec{\Psi}(x)$ is given by

$$\vec{\Psi}(x) = (\psi_{210}(x), \psi_{211}(x), \psi_{212}(x), \psi_{213}(x), \psi_{220}(x), \psi_{221}(x), \psi_{222}(x), \psi_{223}(x)).$$

The step size for the collocation points, $\Delta z = \Delta u$, depends on the length of the vector $\vec{\Psi}$ and is given by

$$\Delta z = \frac{1}{n_{km}} = \frac{2^{1-k}}{m}.$$

The collocation points are defined as

$$z_1 = \frac{\Delta z}{2}, \quad z_i = z_{i-1} + \Delta z, \quad u_1 = \frac{\Delta u}{2}, \quad u_i = u_{i-1} + \Delta u, \quad i = 2, 3, \ldots, n_{km}. \tag{2.6}$$

To approximate the fractional derivatives (in the Caputo sense) of orders β and γ, we use wavelet-based approximations:

$$\frac{\partial^\gamma W}{\partial u^\gamma} \approx \frac{1}{\Gamma[1-\gamma]}\vec{\Psi}(z)\cdot M_1 \cdot \int_0^u \frac{\vec{\Psi}(u')\,du'}{(u-u')^\gamma}, \tag{2.7}$$

and

$$\frac{\partial^\beta W}{\partial z^\beta} \approx \frac{1}{\Gamma[1-\beta]}\int_0^z \frac{\vec{\Psi}(z')\,dz'}{(z-z')^\beta}\cdot M_2 \cdot \vec{\Psi}(u). \tag{2.8}$$

The numerical solution can then be expressed as

$$W_1(z,u) = \vec{\Psi}(z)\cdot M_1 \cdot \int_0^u \vec{\Psi}(u')\,du' + V_1 \cdot \vec{\Psi}(z), \tag{2.9}$$

and

$$W_2(z,u) = \int_0^z \vec{\Psi}(z')\,dz' \cdot M_2 \cdot \vec{\Psi}(u) + V_2 \cdot \vec{\Psi}(u). \tag{2.10}$$

All integrals in the above approximations are computed exactly due to the linear dependence of the wavelets on the Euler polynomials E_m.

Using the definitions in Equations (5) and (6), we formulate the system of algebraic equations to be solved:

$$\begin{cases} d_1\frac{\partial^\beta W(z_i,u_j)}{\partial z^\beta} + d_2\frac{\partial^\gamma W(z_i,u_j)}{\partial u^\gamma} = h(z_i,u_j), \\ W_1(z_i,u_j) = W_2(z_i,u_j), \\ W_1(z_i,0) = k_1(z_i), \\ W_2(0,u_j) = k_2(u_j), \end{cases} \tag{2.11}$$

for $i = 1, 2, \ldots, n_{km}$ and $j = 1, 2, \ldots, n_{km}$. This system of linear equations can be solved using standard solvers, such as those implemented in Mathematica version 14.2.

3. Proposition and Theoretical Justification

Drawing on the numerical results discussed in Section 4, we state a proposition that captures the observed behavior of zero absolute error for a particular class of polynomial solutions. Specifically, this result holds when the exact solution can be expressed as a linear combination of monomials in z and u with rational coefficients, and both the fractional differentiation and wavelet projections are performed symbolically.

Theorem 3.1 *Let*

$$W(z,u) = \sum_{i=0}^{6} a_i z^i + \sum_{j=0}^{6} b_j u^j, \quad \text{with } a_i, b_j \in \mathbb{Q}, \tag{3.1}$$

and let $\beta, \gamma \in (0,1) \cap \mathbb{Q}$. Consider the fractional advection equation:

$$d_1 \frac{\partial^\beta W}{\partial z^\beta} + d_2 \frac{\partial^\gamma W}{\partial u^\gamma} = h(z,u), \tag{3.2}$$

where

$$h(z,u) = d_1 \sum_{i=1}^{6} a_i \cdot \frac{i!}{\Gamma(i+1-\beta)} z^{i-\beta} + d_2 \sum_{j=1}^{6} b_j \cdot \frac{j!}{\Gamma(j+1-\gamma)} u^{j-\gamma}. \tag{3.3}$$

Assume the following:

- *The Euler wavelet basis is used with parameters $k = 2$, $m = 6$, and $n_{km} = 12$.*
- *The collocation points are rational, given by $z_i = \left(i - \frac{1}{2}\right)\Delta z$, $u_j = \left(j - \frac{1}{2}\right)\Delta u$, with $\Delta z = \Delta u = \frac{1}{12}$.*
- *All computations are carried out using symbolic or rational arithmetic.*

Then, the Euler wavelet collocation method produces a numerical solution $\tilde{W}(z_i, u_j)$ that exactly matches the analytic solution:

$$\tilde{W}(z_i, u_j) = W(z_i, u_j), \quad \forall\, i, j = 1, \ldots, 12. \tag{3.4}$$

Proof: From fractional calculus, the Caputo derivative of x^n for $n \in \mathbb{N}$, $\alpha \in (0,1)$ is:

$${}^C D_x^\alpha x^n = \begin{cases} 0, & n = 0, \\ \dfrac{\Gamma(n+1)}{\Gamma(n+1-\alpha)} x^{n-\alpha}, & n \geq 1. \end{cases} \tag{3.5}$$

Using this, we compute:

$${}^C D_z^\beta W = \sum_{i=1}^{6} a_i \cdot \frac{\Gamma(i+1)}{\Gamma(i+1-\beta)} z^{i-\beta}, \quad {}^C D_u^\gamma W = \sum_{j=1}^{6} b_j \cdot \frac{\Gamma(j+1)}{\Gamma(j+1-\gamma)} u^{j-\gamma}. \tag{3.6}$$

Since $W(z,u)$ is a polynomial of degree ≤ 6 in each variable, it is exactly representable in the Euler wavelet basis with $k = 2$, $m = 6$:

$$W(z,u) = \sum_{i=1}^{12} \sum_{j=1}^{12} c_{ij} \psi_i(z) \phi_j(u). \tag{3.7}$$

Fractional differentiation matrices built symbolically (via rational Caputo integrals) yield exact derivatives at collocation points:

$$d_1 \, {}^C D_z^\beta \tilde{W}(z_i, u_j) + d_2 \, {}^C D_u^\gamma \tilde{W}(z_i, u_j) = h(z_i, u_j). \tag{3.8}$$

Because W and $\tilde{W}$ belong to the same function space and satisfy the same linear system, it follows that:

$$\tilde{W}(z_i, u_j) = W(z_i, u_j), \quad \forall\, i, j. \tag{3.9}$$

□

Remark 3.1 *Although this theorem focuses on polynomial solutions of degree ≤ 6 with rational coefficients, numerical results from Section 4 (Code Validation) indicate the Euler wavelet method maintains nearly exact accuracy for a much broader class of smooth solutions. This behavior encourages future theoretical work to establish broader exactness and convergence guarantees.*

4. The Symbolic Accuracy

In a preceding result (see Theorem 3.1), we established that the Euler wavelet collocation method yields zero absolute error when the exact solution is a polynomial of degree less than or equal to six. This section provides a more general theoretical justification that applies to any polynomial solution of degree at most m, where m is the order of the Euler wavelet basis. The following theorem explains why the proposed numerical method produces exact values at all collocation points in such cases.

Theorem 4.1 *Let $m, k \in \mathbb{N}$, and define $n_{km} = 2^{k-1}m$. Consider the Euler wavelet basis of order m and level k defined on the interval $[0, 1]$, with collocation points given by*

$$z_i = \left(i - \tfrac{1}{2}\right)\Delta z, \quad u_j = \left(j - \tfrac{1}{2}\right)\Delta u, \quad \text{where } \Delta z = \Delta u = \frac{1}{n_{km}}, \quad 1 \leq i, j \leq n_{km}. \tag{4.1}$$

Let $\beta, \gamma \in (0, 1) \cap \mathbb{Q}$ denote the fractional orders of differentiation in the Caputo sense, and let $d_1, d_2 \in \mathbb{Q}$ be fixed transport coefficients.

Suppose the exact solution is given by a polynomial of the form

$$W(z, u) = \sum_{i=0}^{n_1} a_i z^i + \sum_{j=0}^{n_2} b_j u^j, \quad \text{with } a_i, b_j \in \mathbb{Q}, \quad n_1, n_2 \leq m, \tag{4.2}$$

and that it satisfies the generalized fractional advection equation

$$d_1 \frac{\partial^\beta W}{\partial z^\beta}(z, u) + d_2 \frac{\partial^\gamma W}{\partial u^\gamma}(z, u) = h(z, u), \tag{4.3}$$

where the right-hand side is explicitly given by

$$h(z, u) = d_1 \sum_{i=1}^{n_1} a_i \cdot \frac{i!}{\Gamma(i + 1 - \beta)} z^{i-\beta} + d_2 \sum_{j=1}^{n_2} b_j \cdot \frac{j!}{\Gamma(j + 1 - \gamma)} u^{j-\gamma}. \tag{4.4}$$

Assume that all symbolic computations—including the construction of the wavelet representation, evaluation of fractional derivatives, matrix assembly, and evaluation at collocation points—are carried out exactly using rational arithmetic. Then, the Euler wavelet collocation method yields a numerical solution $\tilde{W}(z_i, u_j)$ that exactly matches the analytic solution at each collocation point:

$$\tilde{W}(z_i, u_j) = W(z_i, u_j), \quad \forall\, i, j = 1, \ldots, n_{km}. \tag{4.5}$$

Proof: Let

$$W(z, u) = \sum_{i=0}^{n_1} a_i z^i + \sum_{j=0}^{n_2} b_j u^j, \quad \text{with } a_i, b_j \in \mathbb{Q}, \quad n_1, n_2 \leq m,$$

be the exact solution to the fractional advection equation described above. This function is separable as $W(z, u) = P(z) + Q(u)$, where $P(z)$ and $Q(u)$ are univariate polynomials of degree at most m. Because the Euler wavelet basis of order m includes all polynomials up to degree m, it follows that:

$$W(z, u) \in \mathcal{V} := \operatorname{span}(\vec{\Psi}(z)) \oplus \operatorname{span}(\vec{\Psi}(u)).$$

Hence, W lies in the space spanned precisely by the wavelet basis used in the numerical scheme.

The Caputo derivative of a monomial x^n is given symbolically by:

$$ {}^{C}D_x^{\alpha} x^n = \frac{\Gamma(n+1)}{\Gamma(n+1-\alpha)} x^{n-\alpha}, \quad n \in \mathbb{N},\ \alpha \in (0,1), $$

so that the fractional derivatives of W can be computed exactly. Since all coefficients a_i, b_j are rational and all powers and constants are symbolic, the resulting $h(z,u)$ is exactly computable symbolically.

The numerical solution constructed by the Euler wavelet method takes the symbolic form:

$$ \tilde{W}(z,u) = \vec{\Psi}(z)^{\top} M \vec{\Psi}(u) + \vec{v}_1^{\top} \vec{\Psi}(z) + \vec{v}_2^{\top} \vec{\Psi}(u), \tag{4.6} $$

where $M \in \mathbb{Q}^{n_{km} \times n_{km}}$ and $\vec{v}_1, \vec{v}_2 \in \mathbb{Q}^{n_{km}}$ arise from solving the symbolic collocation system.

This structure reflects the formulation of W_1 and W_2, defined in equations (2.9) and (2.10), which construct the solution via fractional integration in one direction:

$$ W_1(z,u) = \vec{\Psi}(z) \cdot M_1 \cdot \int_0^u \vec{\Psi}(u')\, du' + V_1 \cdot \vec{\Psi}(z), \tag{4.7} $$

$$ W_2(z,u) = \int_0^z \vec{\Psi}(z')\, dz' \cdot M_2 \cdot \vec{\Psi}(u) + V_2 \cdot \vec{\Psi}(u). \tag{4.8} $$

To match both approximations and satisfy the boundary conditions (equation (2.11)), the symbolic solver produces a unified form for $\tilde{W}(z,u)$ that includes both bilinear and univariate wavelet terms.

At each rational collocation point (z_i, u_j), the symbolic system enforces:

$$ d_1\, {}^{C}D_z^{\beta} \tilde{W}(z_i,u_j) + d_2\, {}^{C}D_u^{\gamma} \tilde{W}(z_i,u_j) = h(z_i,u_j), $$

along with:

$$ W_1(z_i,u_j) = W_2(z_i,u_j), \quad W_1(z_i,0) = k_1(z_i), \quad W_2(0,u_j) = k_2(u_j). $$

Since all basis functions, fractional derivatives, and collocation values are rational or symbolic, the system becomes a linear symbolic system over $\mathbb{Q}$, with a unique solution for the coefficients M, $\vec{v}_1$, and $\vec{v}_2$. Moreover, the original function W, which is on the same basis and satisfies the same conditions, must also satisfy the same symbolic system. By the uniqueness of solutions to symbolic linear systems, it follows that:

$$ \tilde{W}(z_i,u_j) = W(z_i,u_j), \quad \forall\, i,j. $$

□

5. Existence and Uniqueness Justification

We now justify the existence and uniqueness of the exact and numerical solutions considered in Theorem 4.1.

Existence and Uniqueness of the Exact Solution. Consider the generalized fractional advection equation:

$$ d_1\, {}^{C}D_z^{\beta} W(z,u) + d_2\, {}^{C}D_u^{\gamma} W(z,u) = h(z,u), \tag{5.1} $$

with boundary conditions:

$$ W(0,u) = k_1(u), \quad W(z,0) = k_2(z), \tag{5.2} $$

where $\beta, \gamma \in (0,1)$, and $d_1, d_2 \in \mathbb{Q}$. Assume that the source term $h(z,u)$ and the boundary data $k_1(u), k_2(z)$ are continuous in the domain $[0,1]^2$.

Under these conditions, the existence and uniqueness of a classical solution are supported by fractional analogues of the Picard-Lindelöf theorem and related results in the theory of Caputo fractional differential equations. Specifically, if the right-hand side $h(z,u)$ is continuous and the fractional derivatives exist and are well defined in the classical or Caputo sense for the class of trial solutions, then a unique solution exists within a suitable function space. In our setting, where W is a polynomial and h is explicitly defined from it, the required smoothness and compatibility conditions are satisfied, and the solution is uniquely determined.

Existence and Uniqueness of the Numerical Solution. The numerical solution $\tilde{W}(z,u)$ is computed by projecting the problem onto the Euler wavelet basis and solving a symbolic collocation system. This system has the form:

$$A\vec{x} = \vec{b},$$

where the matrix $A \in \mathbb{Q}^{N\times N}$ is constructed from evaluations of the Euler wavelet basis functions and their symbolic integrals at rational collocation points (z_i, u_j). The unknown vector $\vec{x}$ contains the entries of the coefficient matrix M and the correction vectors $\vec{v}_1, \vec{v}_2$, while $\vec{b}$ contains evaluations of $h(z,u)$ and boundary conditions at collocation points.

Because:

- The Euler wavelet basis functions $\vec{\Psi}$ are linearly independent,
- The collocation grid has size $n_{km} \times n_{km}$, equal to the number of basis functions,
- All entries of A and $\vec{b}$ are computed symbolically in rational arithmetic,

the matrix A is non-singular, and the system has a unique symbolic solution over $\mathbb{Q}$. This guarantees that the numerical approximation $\tilde{W}(z,u)$ exists and is uniquely defined in the Euler wavelet space.

6. Algorithm Validation

To evaluate the efficiency of the numerical method described above, we used an exact solution to the problem (1-2) in the special case where

$$k_1 = z^2, \quad k_2 = u^2, \quad h = d_1\frac{z^{2-\beta}}{\Gamma(3-\beta)} + d_2\frac{u^{2-\gamma}}{\Gamma(3-\gamma)}. \tag{6.1}$$

The exact solution is given by $W = z^2 + u^2$. We computed the numerical solution using a wavelet basis with $k = 2$, $m = 4$, and $n_{km} = 8$ in the range $\frac{1}{10} \le \beta \le \frac{9}{10}$ and $\frac{1}{10} \le \gamma \le \frac{9}{10}$, with a step size of $\frac{1}{10}$. The parameters d_1 and d_2 were set to $\frac{1}{2}$ and 2, respectively. The maximal absolute error for this test was approximately 10^{-15} for runs with machine precision and less than 10^{-40} for all runs with double precision (see Figure 1).

The second test was performed using the exact solution proposed in [30] for the special case $\beta = \gamma = \frac{1}{2}$ and for

$$d_1 = d_2 = \sqrt{\pi}, \quad k_1 = z^2, \quad k_2 = u^2, \quad h = \frac{8z^{3/2}}{3} + \frac{8u^{3/2}}{3}. \tag{6.2}$$

As in the previous case, the exact solution is given by $W = z^2 + u^2$. Numerical solutions were calculated with double precision using two wavelet bases: one with $k = 2$, $m = 4$, $n_{km} = 8$ and another with $k = 3$, $m = 4$, $n_{km} = 16$ (see Figure 1). In both grids, the absolute error was less than 10^{-40} (Figure 1, bottom line).

We performed several additional tests to estimate the absolute error using exact solutions given by

$$W = z^{n_1} + u^{n_2}, \quad h = d_1\frac{n_1! z^{n_1-\beta}}{\Gamma(n_1+1-\beta)} + d_2\frac{n_2! u^{n_2-\gamma}}{\Gamma(n_2+1-\gamma)}, \tag{6.3}$$

for different combinations of $n_1 = 1,2,3,4,5,6,7,8,9$ and $n_2 = 1,2,3,4,5,6,7,8,9$, with fixed $d_1 = d_2 = 1$ and $\beta = \gamma = \frac{1}{4}, \frac{1}{2}, \frac{2}{3}, \frac{3}{4}$ (see Figure 2). For these solutions, we observed a zero maximal absolute error for all combinations of $n_1 = 1,2,3,4$ with $n_2 = 1,2,3,4$ and for $\beta = \gamma = \frac{1}{4}, \frac{1}{2}, \frac{2}{3}, \frac{3}{4}$. However, for $n_1 \ge 5$ or $n_2 \ge 5$, the precision of the numerical solution suddenly drops, resulting in a maximal absolute error of up to 10^{-3} (see Figure 3). Increasing the calculation accuracy to 60 digits did not significantly improve the results, as the maximal absolute error only decreased to 10^{-4}.

It can be assumed that this deterioration in the accuracy of the numerical solution is related to the use of the proposed algorithm with a wavelet base limited to $k = 2$, $m = 4$, and $n_{km} = 8$. To investigate this, we performed a numerical error analysis for $n_1 = n_2 = 5$ using numerical fractional differentiation matrices and several wavelet bases with $n_{km} = 6, 8, 10, 12, 14, 16, 20, 24$ (see Figure 4). We calculated the

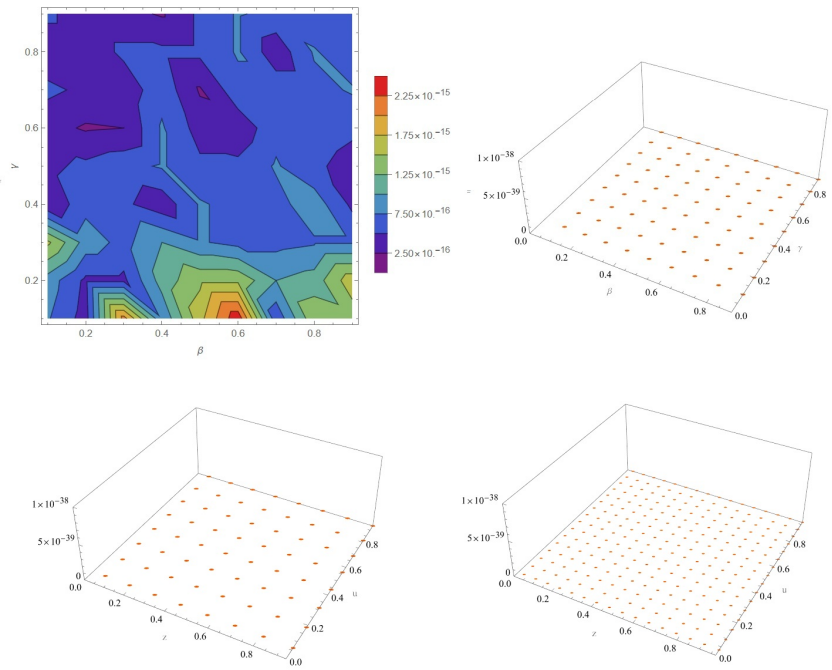

Figure 1: The maximal absolute error vs β, γ computed for exact solutions (8) with machine precision (top, left) and with double precision (top, right); absolute error vs z, u calculated for exact solution (9) at $n_{km} = 8$ (bottom, left) and $n_{km} = 16$ (bottom, right).

convergence rate using these data, which was approximately 7.88. It is worth noting that a convergence rate of about 8 is common in numerical computations using Euler wavelets. The absolute error distribution shown in Figure 4 shows flat regions corresponding to a very low absolute error. Therefore, this case can also be addressed using a different wavelet base, such as $k = 2$, $m = 6$, $n_{km} = 12$. By generating an exact fractional differentiation matrix, we achieved zero absolute error for different combinations of $n_1 = 1, 2, 3, 4, 5, 6$ with $n_2 = 1, 2, 3, 4, 5, 6$ and fixed $d_1 = d_2 = 1$, $\beta = \gamma = \frac{1}{4}, \frac{1}{2}, \frac{2}{3}, \frac{3}{4}$ (see Figure 5). However, for $n_1 \geq 7$ or $n_2 \geq 7$, the absolute error was approximately 10^{-5}. To address this, an exact fractional differentiation matrix should be generated in the Euler wavelet base with $m \geq 7$.

The next examples show that we can combine series with $0 \leq n_1 \leq 6, \quad 0 \leq n_2 \leq 6$ and with arbitrary rational coefficient $a_i, b_i, i = 0, 1, ..., 6$ so that exact solution and function h are given by

$$W = \sum_{i=0}^{n_1} a_i z^i + \sum_{i=0}^{n_2} b_i u^i, \quad h = d_1 \sum_{n=1}^{n_1} \frac{a_n n! z^{n-\beta}}{\Gamma(n+1-\beta)} + d_2 \sum_{n=1}^{n_2} \frac{b_n n! u^{n-\gamma}}{\Gamma(n+1-\gamma)} \tag{6.4}$$

Using exact fractional differentiation matrix at $k = 2, m = 6, n_{k,m} = 12$, we have been able to compute numerical solution with zero absolute error, for example (14) with coefficient

$$a = \left(0, 0, \tfrac{1}{7}, \tfrac{6}{7}, 0, 0, \tfrac{2}{7}\right), \quad b = \left(0, 0, 0, \tfrac{4}{5}, 1, 1, \tfrac{2}{5}\right). \tag{6.5}$$

The exact solution and the corresponding error over the range $\frac{1}{10} \leq \beta \leq \frac{9}{10}$ and $\frac{1}{10} \leq \gamma \leq \frac{9}{10}$, with a step size of $\frac{1}{10}$, are shown in Figure 6 (left). Notably, the point computed at $\beta = \frac{7}{10}, \gamma = \frac{4}{5}$ exhibits the largest absolute error of 8.94×10^{-30}, while all other computations result in errors smaller than 10^{-40}.

In the final example, the same parameter range was considered— $\frac{1}{10} \leq \beta \leq \frac{9}{10}$, $\frac{1}{10} \leq \gamma \leq \frac{9}{10}$—but

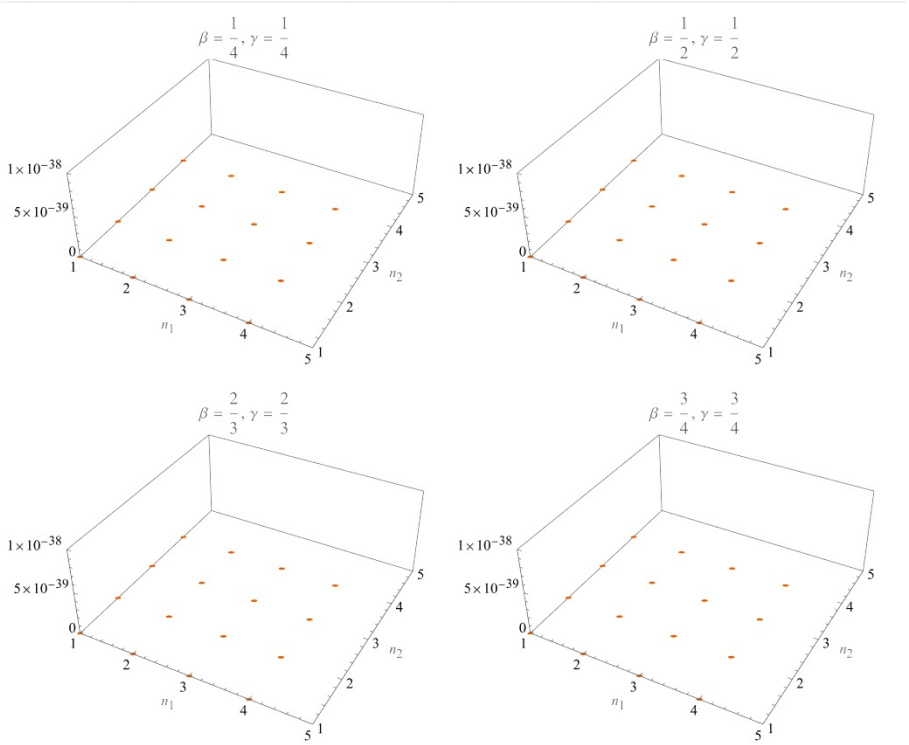

Figure 2: The maximal absolute error computed with double precision for exact solution (10).

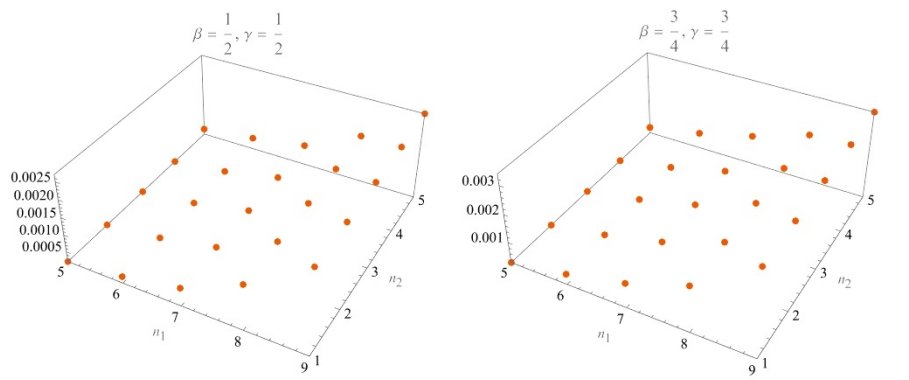

Figure 3: The maximal absolute error for exact solution (8) with $n_1 \geq 5$ and $1 \leq n_2 \leq 5$.

k	m	n_{km}	δW_{max}
2	3	6	0.00230241
2	4	8	0.000368767
2	5	10	1.22147×10^{-8}
2	6	12	4.29514×10^{-9}
2	7	14	3.9858×10^{-9}
3	4	16	0.0000171557
3	5	20	1.03713×10^{-8}
3	6	24	1.48663×10^{-8}

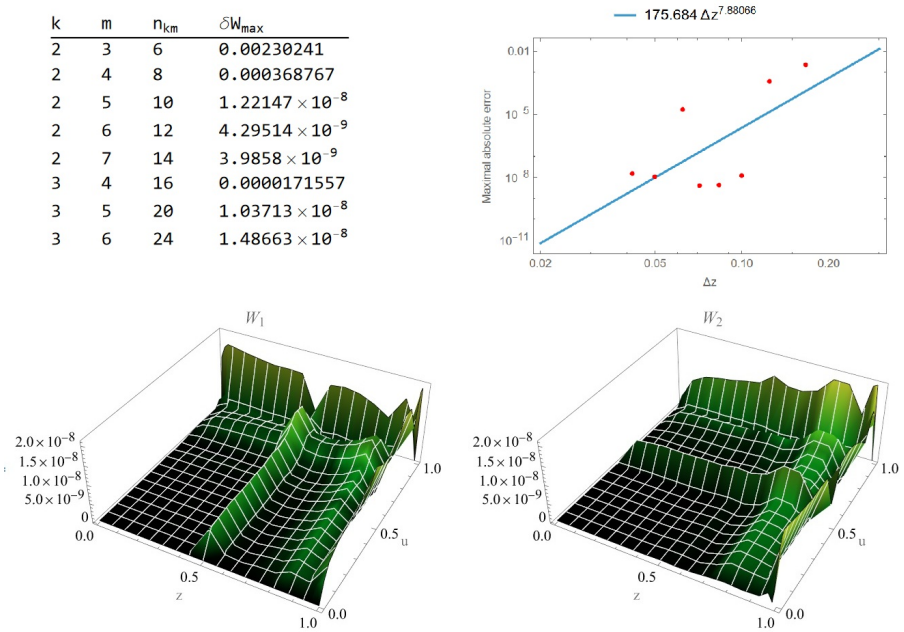

Figure 4: Maximal absolute error computed for 8 wavelet bases (top, left), the convergence rate (top, right), and the distribution of the maximal absolute error at $n_{km} = 24$ for the numerical solutions W_1 (bottom, left) and W_2 (bottom, right).

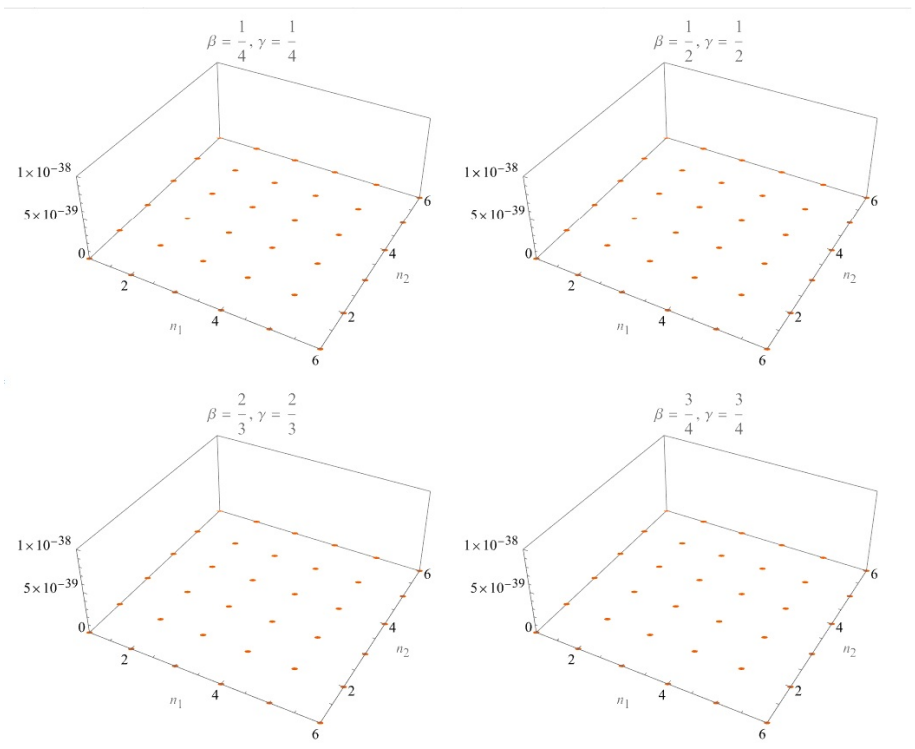

Figure 5: The maximal absolute error computed with double precision for exact solution (10) at $k = 2$, $m = 6$, $n_{km} = 12$.

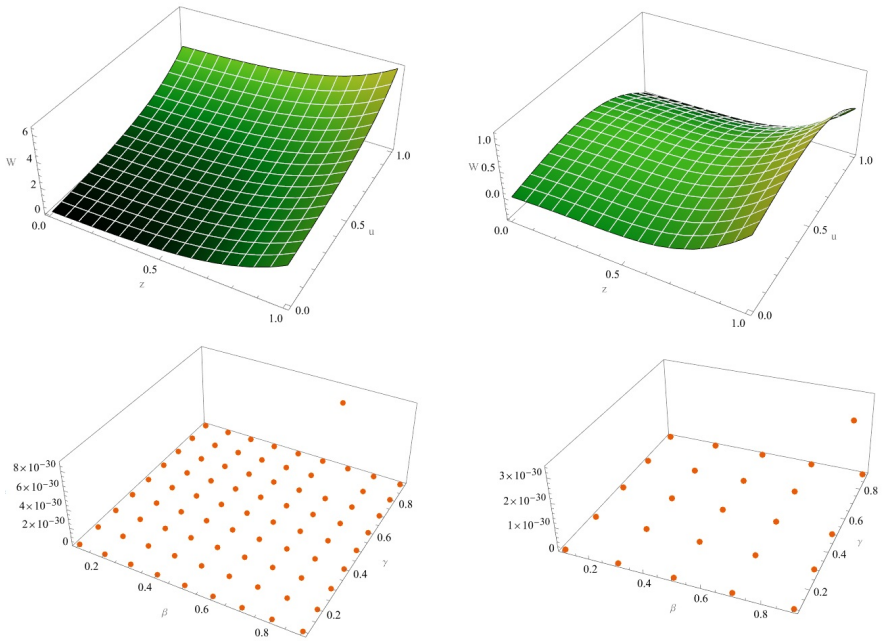

Figure 6: The exact solution and the maximal absolute error computed with double precision at $k = 2$, $m = 6$, $n_{km} = 12$ for (14),(15) - left, and for (14),(16) - right.

with a step size of $\frac{1}{5}$. The coefficients used were:

$$\begin{aligned} a &= \left(0, \frac{32708048}{186874227}, -\frac{11283656}{136484857}, -\frac{110035602}{108025985}, \frac{28226629}{27151850}, \frac{74410621}{38356544}, -\frac{177109294}{156481923}\right), \\ b &= \left(0, \frac{57240248}{75994367}, \frac{14872377}{338558723}, -\frac{23556129}{28464793}, -\frac{118460031}{485145784}, -\frac{74401801}{76175872}, \frac{81062132}{94861399}\right). \end{aligned} \tag{6.6}$$

The corresponding exact solution and the maximum absolute error are shown in Figure 6 (right). Once again, the largest error—approximately 3.45×10^{-30}—occurs at $\beta = \frac{9}{10}, \gamma = \frac{7}{10}$, while all other results remain below 10^{-40}.

These examples demonstrate the great potential of the proposed method. A numerical solution with very low error can be obtained for functions that can be expressed as a series. This statement can be formulated as a theorem.

7. Conclusion

This work presented an Euler wavelet collocation method for numerically solving time–space fractional advection equations involving Caputo derivatives. The approach combines the compact support and polynomial precision of Euler polynomials with the multiresolution structure of wavelets, resulting in a numerical framework well-suited to non-local PDEs.

A key contribution of this study is the theoretical demonstration-under exact rational arithmetic-that the proposed method yields pointwise-exact solutions at collocation nodes when the exact solution is polynomial. This was established through a rigorous symbolic framework, ensuring that all operations, including fractional derivatives and matrix construction, are carried out with full precision. The main theorem confirms that, for a class of analytic inputs, the Euler wavelet method exactly reproduces the true solution, underscoring its suitability for problems where symbolic integrity is critical.

Beyond this theoretical guarantee, the method also addresses a broader class of problems than many existing works, which are often limited to either time-fractional formulations or integer-order systems.

In contrast, the present model incorporates fractional orders in both spatial variables, enabling a more complete description of anomalous transport behavior.

From a computational perspective, the method exhibits high accuracy and efficiency, particularly for problems with smooth solutions, where the collocation strategy combined with the Euler basis yields rapid convergence. The successful handling of both boundary conditions and fractional derivatives within a unified framework further strengthens the method's applicability.

Future directions include extending the method to nonlinear or multi-dimensional systems, as well as exploring adaptive grid strategies and symbolic-numeric hybrid solvers. Given its precision and theoretical soundness, the Euler wavelet framework provides a strong foundation for advancing the numerical treatment of space–time fractional PDEs in both applied and theoretical settings.

Acknowledgments

We sincerely thank the referee for their valuable suggestions, which have greatly helped improve the clarity and quality of our work.

References

1. P. AGARWAL, A. M. A. EL-SAYED, AND J. TARIBOON, *Vieta-fibonacci operational matrices for spectral solutions of variable-order fractional integro-differential equations*, J. Comput. Appl. Math., 382 (2021), p. 113063.

2. J. ALVAREZ AND Y. WANG, *Euler wavelet method as a numerical approach for fractional integro-differential optimal control problems*, J. Comput. Appl. Math., 418 (2024), p. 116178.

3. W. CHEN AND S. HOLM, *Wavelet methods for fractional partial differential equations*, Signal Processing, 83 (2003), pp. 2359–2367.

4. J. CHOI, P. AGARWAL, AND S. JAIN, *Certain fractional integral operators and extended generalized gauss hypergeometric functions*, Kyungpook Mathematical Journal, 55 (2015), pp. 695–703.

5. F. DE LA HOZ AND P. MUNIAIN, *Numerical approximation of caputo-type advection-diffusion equations via sylvester equations*, arXiv, 2501.09180 (2025).

6. K. DIETHELM, *The Analysis of Fractional Differential Equations: An Application-Oriented Exposition Using Differential Operators of Caputo Type*, Springer, 2010.

7. A. A. EL-SAYED, D. BALEANU, AND P. AGARWAL, *A novel jacobi operational matrix for numerical solution of multi-term variable-order fractional differential equations*, Journal of Taibah University for Science, 14 (2020), pp. 963–974.

8. A. ELAHI, S. IRANDOUST-PAKCHIN, A. RAHIMI, AND S. ABDI-MAZRAEH, *A new approach of b-spline wavelets to solve fractional differential equations*, Communications in Nonlinear Science and Numerical Simulation, 136 (2024), p. 108099.

9. J. F. GÓMEZ AGUILAR AND M. M. HERNÁNDEZ, *Space-time fractional diffusion-advection equation with caputo derivative*, Abstract Appl. Anal., 2014 (2014), p. 283019.

10. M. M. KHADER, M. ADEL, AND T. A. ABASSY, *A new operational wavelet method for solving fractional differential equations with variable coefficients*, Mathematics, 8 (2020), p. 406.

11. A. A. KILBAS, H. M. SRIVASTAVA, AND J. J. TRUJILLO, *Theory and Applications of Fractional Differential Equations*, Elsevier, 2006.

12. İ. KIYMAZ, P. AGARWAL, S. JAIN, AND A. ÇETINKAYA, *On a New Extension of Caputo Fractional Derivative Operator*, Springer Singapore, Singapore, 2017, pp. 261–275.

13. C. LI AND Y. ZHAO, *A wavelet-galerkin method for solving fractional differential equations*, Applied Mathematics and Computation, 215 (2010), pp. 3118–3128.

14. F. MAINARDI, *Fractional Calculus and Waves in Linear Viscoelasticity*, Imperial College Press, 2010.

15. M. M. MEERSCHAERT, D. A. BENSON, AND B. BAEUMER, *Modeling anomalous diffusion with fractional advection-dispersion equations*, Physica A: Statistical Mechanics and its Applications, 302 (2001), pp. 234–241.

16. R. METZLER AND J. KLAFTER, *The random walk's guide to anomalous diffusion: a fractional dynamics approach*, Physics Reports, 339 (2000), pp. 1–77.

17. M. MOHAMMAD, *Cognitive AI and implicit pseudo-spline wavelets for enhanced seismic prediction*, International Journal of Cognitive Computing in Engineering, 6 (2025), pp. 401–411.

18. M. MOHAMMAD, *A tight wavelet frames-based method for numerically solving fractional riccati differential equations*, Mathematical Methods in the Applied Sciences, (2025).

19. M. MOHAMMAD AND M. SAADAOUI, *A new fractional derivative extending classical concepts: Theory and applications*, Partial Differential Equations in Applied Mathematics, 11 (2024), p. 100889.

20. M. Mohammad and A. Trounev, *On the dynamical modeling of COVID-19 involving Atangana–Baleanu fractional derivative and based on Daubechies framelet simulations*, *Chaos, Solitons & Fractals*, 140 (2020), 110171.

21. M. Mohammad and A. Trounev, *Explicit tight frames for simulating a new system of fractional nonlinear partial differential equation model of alzheimer disease*, Results in Physics, 21 (2021), p. 103809.

22. M. Mohammad and A. Trounev, *A new technique for solving neutral delay differential equations based on euler wavelets*, Complexity, 2022 (2022), p. 1753992.

23. M. Mohammad and A. Trounev, *An advanced algorithm for solving incompressible fluid dynamics: from navier–stokes to poisson equations*, The European Physical Journal Special Topics, (2024).

24. M. Mohammad and A. Trounev, *Computational precision in time fractional pdes: Euler wavelets and novel numerical techniques*, Partial Differential Equations in Applied Mathematics, 12 (2024), p. 100918.

25. M. Mohammad, A. Trounev, and C. Cattani, *The dynamics of covid-19 in the uae based on fractional derivative modeling using riesz wavelets simulation*, Advances in Difference Equations, 2021 (2021), p. 115.

26. S. K. Ntouyas, P. Agarwal, and J. Tariboon, *On pólya–szegő and chebyshev types inequalities involving the riemann–liouville fractional integral operators*, Journal of Mathematical Inequalities, 10 (2016), pp. 491–504.

27. I. Podlubny, *Fractional Differential Equations*, Academic Press, 1999.

28. G. Singh, P. Agarwal, M. Chand, and S. Jain, *Certain fractional kinetic equations involving generalized bessel function*, Transactions of A. Razmadze Mathematical Institute, 172 (2018), pp. 559–570.

29. A. Soltanpour Moghadam and M. Arabameri, *An explicit finite difference approximation for space–time riesz–caputo variable order fractional wave equation*, Numer. Anal. Appl., 17 (2024), pp. 262–275.

30. M. Zayernouri and G. E. Karniadakis, *Discontinuous spectral element methods for time- and space-fractional advection equations*, SIAM Journal on Scientific Computing, 36 (2014), pp. B684–B707.

31. H. Zhang, F. Li, and M. Zhang, *High-order numerical approximation for 2d time-fractional advection–diffusion equation*, Fractal Fract., 8 (2024), p. 474.

32. X. Zhang, P. Agarwal, Z. Liu, and H. Peng, *The general solution for impulsive differential equations with Riemann-Liouville fractional-order $q \in (1, 2)$*, *Open Mathematics*, 13 (2015), 000010151520150073.

Mutaz Mohammad,
Department of Mathematics,
Zayed Univeristy,
UAE.
E-mail address: Mutaz.Mohammad@zu.ac.ae

and

Mohyeedden Sweidan,
Department of Mathematics,
Concord University,
USA.
E-mail address: msweidan@concord.edu

and

Alexander Trounev,
Kuban State Agrarian University,
Russia.
E-mail address: trounev.a@edu.kubsau.ru

and

P.Agrawal,
Department of Mathematical Sciences,
Saveetha School of Engineering, Chennai, Tamil Nadu, 602105, India
Nonlinear Dynamics Research Center (NDRC), Ajman University, Ajman, UAE
Department of Mathematics,
Anand International College of Engineering, Jaipur 303012, India.
E-mail address: goyal.praveen2011@gmail.com